A CASSCF Study on Photodissociation of Acrolein in the Gas Phase

Wei-Hai Fang*

Contribution from the Department of Chemistry, Beijing Normal University, Beijing 100875, P. R. China, and Institut für Physikalische und Theoretische Chemie, Universität Bonn, Wegelerstrasse 12, 53115 Bonn, Germany

Received July 3, 1998

Abstract: The potential energy profiles, governing the dissociation of CH_2CHCHO to $CH_3CH + CO$, $CH_2CH + CHO$, and $CH_2CHCO + H$ in the ground state as well as in the excited singlet and triplet states, have been determined using different ab initio quantum mechanical methods with a correlation-consistent atomic natural orbital basis set, cc-pVDZ. The most probable mechanism leading to different products is characterized on the basis of the obtained potential energy profiles and their crossing points. Also, the geometric and electronic structures of some low-lying electronic states of acrolein, methylketene, methylcarbene, and the CH_2CHCO radical are determined by the CASSCF computations.

1. Introduction

Molecular photodissociations have long been regarded as an intellectually challenging, but potentially tractable, area of chemical physics, the results of which are relevant to atmospheric chemistry (especially the chemistry of planetary atmospheres), biological systems (enzymes, genes, and antibodies), and many other processes.[1,2] Recent advances in experimental techniques have led to unprecedented progress in the level and detail of our understanding of molecular photodissociation processes.[3,4] Meanwhile, a great leap forward in the ability to carry out quantum mechanical calculations of photochemical processes has been witnessed in the past decade. However, due to the great diversity of possible photoreactions (isomerization, dissociation, hydrogen abstraction, etc.) as well as to the complexity of the product mixtures occurring in the photochemical reactions, it is difficult to provide detailed mechanisms of the photoreactions. Calculations to date have mainly been performed for small molecules, such as HCO,[5] H_2CO,[6] HONO,[7] HNCO,[8] and CH_3NH_2,[9] and for some larger molecules,[10,11] and still our understanding of the photochemistry of these molecules remains far from complete.

The gas-phase photochemistry of small aldehydes has been the subject of numerous experimental investigations and has been reviewed by several authors.[12,13] Acrolein (CH_2CHCHO) is one of the smallest unsaturated carbonyl compounds. It is of unique spectroscopic and theoretical interest, because of the interaction between the carbonyl group and the C=C double bond. Early experimental studies mainly concentrated on its spectrum and structure. Walsh[14] observed six absorption bands at different wavelengths. A very weak absorption system starting at 412 nm and a stronger one at 387 nm were assigned to the $n\rightarrow\pi^*$ transition from S_0 to the T_1 and S_1 states, respectively. A stronger and diffuse absorption at shorter wavelengths was also observed, having a maximum near 193.5 nm. This band corresponds to the $\pi\rightarrow\pi^*$ transition. Further spectroscopic investigations[15−18] had provided much information on the $n\pi^*$ state. From emission spectra and theoretical considerations, Becker et al.[17] suggested that photoexcitation of acrolein leads to the $^1n\pi^*$ state (absorption maximum at 330.5 nm), where the fluorescence (375- and 392-nm maxima) of this compound is produced. The fluorescence is obtained with low yield due to fast internal conversion to S_0 or intersystem crossing to the $^3\pi\pi^*$ state that lies very close to S_1.

In addition to a few investigations of the ground-state acrolein,[19−24] several experiments have been done in order to elucidate the photochemical reactions of acrolein.[17,25−30] Trying to demonstrate cis−trans photoisomerization, Becker et al.[17]

* Present address: Department of Chemistry, Beijing Normal University.

(1) Rowland, F. S. *Annu. Rev. Phys. Chem.* **1991**, *42*, 731.
(2) Cantor, C. R.; Schimmel, P. R. *Biophysical Chemistry I*; Freemann: San Francisco, CA, 1980.
(3) Bortolus, P.; Monti, S. *Adv. Photochem.* **1995**, *21*, 218.
(4) Schinke, R. *Annu. Rev. Phys. Chem.* **1988**, *39*, 39.
(5) (a) Goldfield, E. M.; Gray, S. K.; Harding, L. B. *J. Chem. Phys.* **1993**, *99*, 5812. (b) Loettgers, A.; Untch, A.; Keller, H.-M.; Schinke, R.; Werner, H.-J.; Bauer, C.; Rosmus, P *J. Chem. Phys.* **1996**, *106*, 3186.
(6) Yamaguchi, Y.; Wesolowski, S. S.; Van Huis T. J.; Schaefer H. F. *J. Chem. Phys.* **1998**, *108*, 5281 and references therein.
(7) Cotting, R.; Huber, J. R. *J. Chem. Phys.* **1996**, *104*, 6208.
(8) (a) Fang, W.-H.; You, X.-Z.; Yin, Z. *Chem. Phys. Lett*. **1995**, 238, 236. (b) Cui, Q.; Morokuma, K. *J. Chem. Phys.* **1998**, *108*, 1452.
(9) Dunn, K. M.; Morokuma, K. *J. Phys. Chem*. **1996**, *100*, 123.
(10) Klessinger, M. *Angew. Chem., Int. Ed. Engl*. **1995**, *34*, 549−551.
(11) Yamamoto, N.; Olivucci, M.; Celani, P.; Bernard, F.; Robb, M. A. *J. Am. Chem. Soc.* **1998**, *120*, 2391−2407 and references therein.
(12) Jackson, W. N.; Okabe, H. *Adv. Photochem.* **1986**, *13*, 1.
(13) Moore, C. B.; Weisshaar, J. C. *Annu. Rev. Phys. Chem*. **1983**, *34*, 525.
(14) Walsh, A. D. *Trans. Faraday Soc.* **1945**, *41*, 498.
(15) Brand, J. C. D.; Williamson, D. G. *Discuss Faraday Soc*. **1963**, *35*, 184.
(16) Hollas, J. M. *Spectrochim. Acta* **1963**, *19*, 1425.
(17) Becker, R. S.; Inuzuka, K.; King, J. *J. Chem. Phys*. **1970**, *52*, 5164.
(18) Osborne, G. A.; Ramsay, D. A. *Can. J. Phys*. **1973**, *51*, 1170.
(19) Cherniak, E. A.; Costain, C. C. *J. Chem. Phys.* **1966**, *45*, 104.
(20) Kuchitsu, K.; Fukuyama, T.; Morino, Y. *J. Mol. Struct*. **1968**, *1*, 463.
(21) Kuchitsu, K.; Fukuyama, T.; Morino, Y. *J. Mol. Struct.* **1969**, *4*, 41.
(22) Blom, C. E.; Bauder, A. *Chem. Phys. Lett.* **1982**, *85*, 55.
(23) Krantz, A.; Goldoforb, T. D.; Lin, C. T. *J. Am. Chem. Soc*. **1972**, *94*, 4022.
(24) Hamada, Y.; Nishimura, Y.; Tsumoi, M. *Chem. Phys*. **1985**, *100*, 365.
(25) Coomber, J. W.; Pitts, J. N. *J. Am. Chem. Soc*. **1969**, *91*, 547.
(26) Shinohara, H.; Nishi, N. *J. Chem. Phys.* **1982**, *77*, 234.
(27) Umstead, M. E.; Shortridge, R. G.; Lin, M. C. *J. Phys. Chem*. **1978**, *82*, 1455.
(28) Fujimoto, G. T.; Umstead, M. E.; Lin, M. C. *J. Chem. Phys*. **1985**, *82*, 3042.

10.1021/ja982334i CCC: $18.00
Published on Web 08/25/1999

considered cis and trans states arising not only from an n→π^* excitation but also from a $\pi\rightarrow\pi^*$ excitation. They concluded that, largely because of potential barriers between cis and trans excited states, photoisomerization did not occur. Coomber and Pitts[25] photolized acrolein at 313 nm in the gas phase and found the products CO and CH_2CH_2, as well as the radical pair CH_2-CH and HCO. Shinohara and Nishi[26] investigated the laser photofragmentation dynamics of an acrolein supersonic molecular beam at 193 nm. CH_2CH and HCO were reported as the only primary products. These researchers suggested that the dissociation probably proceeds on the S_1 potential energy surface after internal conversion of the S_2 to the S_1 state. The photofragmentation dynamics of the two C_3H_4O isomers, methylketene(CH_3CHCO) and acrolein (CH_2CHCHO), was investigated by Lin et al.[27,28] From the similarities observed in the appearance times and in the vibrational energy content of the CO formed in the two systems, this group came to the conclusion that, in the case of acrolein, isomerization to methylketene takes place prior to the dissociation process: CH_2-$CHCHO \rightarrow CH_3CHCO \rightarrow CH_3CH + CO$. The translational energy distribution and the fragment anisotropy for the 193-nm photodissociation products of acrolein have been measured by Huber and co-workers[29] with a molecular beam time-of-flight technique. Three distinct dissociation pathways have been identified: the molecular channel leading to $CH_2CH_2 + CO$, the radical channel creating $CH_2CH + HCO$, and the hydrogen channel involving the aldehyde C−H bond fission with the products $CH_2CHCO + H$. They speculated that the dissociation processes in acrolein after 193-nm excitation proceed via predissociation, giving rise to a strong participation of the internal degrees of freedom. Recently, Arendt et al.[30] have investigated the emission spectra of the excited-state acrolein, acrylic acid, and acryloyl chloride and pointed out that the photodissociation of compounds with a C═C−C═O backbone does not proceed through a single, direct dissociation mechanism. Rather, it would seem that excitation is initially to a predissociative state from which the dissociation channels are accessible. It is evident that the experimental investigations mentioned above provide distinct information on the mechanism of the reaction, which stimulated our interest in performing an extensive ab initio study of the CH_2CHCHO photodissociation.

Acrolein has also been the subject of many theoretical calculations. The ground-state structure and vibrational frequencies have been studied using semiempirical[31] and ab initio methods.[23,32,33] The experimental data were reproduced well by these ab initio calculations. Unlike the case for the ground state, it seems that there has been some controversy over the excited-state structures, especially the structures of the $\pi\pi^*$ states. The two lowest triplet states have been investigated by Devaquet and Salem[34] and later by Devaquet[35] at the Hartree−Fock SCF level. Large-scale ab initio CI energies of the low-lying states were plotted as a function of the twist angle of the terminal CH_2 group.[36] Unfortunately, the C═C, C−C, and C═O bond lengths were not varied independently, so the molecular structures and relative energies of the states are only qualitatively determined. The SCF calculations of Dykstra[37,38] predicted that the ground and lowest excited singlet and triplet states are planar. This idea has been supported by the CI calculations of Valenta and Grein.[39] However, the nonorthogonal SCF calculations of Davidson and Nitzsche[40] gave the biradical $\dot{C}H_2-\dot{C}H-CH{=}O$ as the $^1\pi\pi^*$ state. The potential energy profile of the CH_2-CHCHO decarbonylation was traced with the ROHF/3-21G method followed by MRSDCI single-point calculations.[41] Recently, an extensive CASSCF study of the CH_2CHCHO photoisomerization was performed by Robb et al.[42] in order to provide a model for understanding the photochemistry and photophysics of α,β-enones. The structures of some crossing points on the ground-state and three low-lying singlet/triplet excited-state surfaces were determined, and a mechanism of photoisomerization reaction was characterized.

Though much experimental effort has been devoted to the study of the CH_2CHCHO photodissociation, as far as I know, very little theoretical information is available for this process. To characterize the mechanism of acrolein photodissociation, a detailed knowledge of ground- and excited-state reaction paths is required. In the present paper, an extensive ab initio calculation has been performed by employing more advanced techniques. The ground- and excited-state potential energy profiles, governing the CH_2CHCHO dissociation to $CH_3CH + CO$, $CH_2CH + CHO$ and $CH_2CHCO + H$, are traced at different levels with a large basis set. Together with the previous experimental and theoretical conclusions, the most probable mechanism of the CH_2CHCHO photodissociation is provided in the present work.

2. Computational Details

Ab initio molecular orbital methods have been used to investigate the ground- and excited-state potential energy surfaces (PESs) of acrolein. The stationary points on the ground-state PES are fully optimized with the MP2(FC), CASSCF, and QCISD(FC) energy gradient techniques, and energies are calculated at the CASSCF-optimized structures with the multireference MP2(CAS-PT2) approach, where FC denotes the frozen 1s core of oxygen and carbon atoms. The CASSCF gradient technique, together with the CIS method, is used to optimize the stationary points on the excited-state potential energy profiles. The selection of the active space is the crucial step in CASSCF calculations. The obvious choice for describing equilibrium structures of acrolein would be six electrons distributed in five orbitals originating from the π and π^* orbitals of the C═C fragment and the π, π^* and n orbitals of the C═O fragment. To characterize the dissociation processes, $CH_2CHCHO \rightarrow CH_2CH + CHO$ and $CH_2CHCHO \rightarrow CH_2$-$CHCO + H$, which involve the breaking of the C−C and C−H σ bonds, respectively, the C−C or C−H σ and σ^* orbitals should be included in the active space. During the processes of rotation and isomerization, π and π^* orbitals are transformed into other types of orbitals which are still used as active orbitals. For a balanced description of the different processes, the active space is composed of eight electrons in seven orbitals, referred to as CAS(8,7). For equilibrium geometries and transition states, the nature of critical points is confirmed by an analytical frequency computation. Geometry optimizations are carried out to the standard convergence criteria, comprised of the following: a maximum element of the gradient of less than 0.00045 hartree/bohr

(29) Haas, B.-M.; Minton, T. K.; Felder, P.; Huber J. R. *J. Phys. Chem.* **1991**, *95*, 5149.
(30) Arendt, M. F.; Browning, P. W.; Butler, L. J. *J. Chem. Phys*. **1995**, *103*, 5877.
(31) Panchenko, Yu. N.; Pulay, P.; Torok, F. *J. Mol. Struct*. **1976**, *34*, 283.
(32) Bock, C. W.; George, P.; Trachtman, M. *J. Mol. Spectrosc*. **1979**, *78*, 298.
(33) Pulay, P.; Fogarasi, G.; Pongor, G.; Boggs, J. E.; Vargha, A. *J. Am. Chem. Soc*. **1983**, *105*, 7037.
(34) Devaquet, A.; Salem, L. *Can. J. Chem*. **1971**, *49*, 977.
(35) Devaquet, A. *J. Am. Chem. Soc*. **1972**, *94*, 5160.
(36) Michl, J.; Bonacic-Koutecky, V. *Electronic Aspects of Organic Photochemistry*; Wiley: New York, 1990, 365−367.
(37) Dykstra, C. E. *J. Am. Chem. Soc.* **1976**, *98*, 7182.
(38) Lucchese, R. R.; Schaefer, H. F.; Dykstra, C. E. *Chem. Phys. Lett*. **1977**, *51*, 600.
(39) Valenta, K.; Grein, F. *Can. J. Chem.* **1982**, *60*, 601.
(40) Davidson, E. R.; Nitzsche, L. E. *J. Am. Chem. Soc.* **1979**, *101*, 6524.
(41) Fang, W.-H.; Huang, M.-B.; Fang, D.-C.; Liu, R.-Z. *J. Mol. Struct. (THEOCHEM)* **1994**, *305*, 185.
(42) Reguero, M.; Olivucci, M.; Bernardi, F.; Robb, M. A. *J. Am. Chem. Soc*. **1994**, *116*, 2103.

(0.54 kcal mol^{-1} Å^{-1}), an RMS of gradient elements of less than 0.0003 hartree/bohr (0.36 kcal mol^{-1}Å^{-1}), a change in energy of less than 0.00001 hartree between final iterations, a maximum nuclear displacement of less than 0.0018 bohr, and an RMS nuclear displacement of less than 0.0012 bohr. After a preliminary search with a 6-31G* basis set, the geometries are further optimized with a correlation-consistent atomic natural orbital basis set, cc-pVDZ.[43] However, only the results obtained with the cc-pVDZ basis set are reported in this paper. All ab initio calculations described here have been performed with the Gaussian 94 program packages.[44]

3. Results and Discussion

Several processes have been proposed experimentally as primary dissociation pathways:

$$CH_2CHCHO + h\nu \rightarrow CH_2CH_2 + CO \quad (1)$$

$$\rightarrow CH_2CH + CHO \quad (2)$$

$$\rightarrow CH_2CHCO + H \quad (3)$$

Reaction 1 is a decarbonylation, referred to as a molecular channel; reaction 2 involves a cleavage of the C−C bond, yielding an acyl and an alkyl radical, which is known as a Norrish type I reaction; reaction 3 gives rise to radical products from the C−H α-cleavage. Acrolein exists in s-trans- and s-cis isomer forms. Both theory and experiment[45,46] agree that, in the ground-state, *s-trans*-acrolein is a more stable isomer, which is used as the initial reactant in the present work.

A. Equilibrium Geometries and Their Electronic Structures. Equilibrium geometry and electronic structure are basic, but very important, properties of a molecule. However, there is a general lack of information on the electronic structures of the excited-state acrolein. Before discussing the photodissociation reactions of acrolein, let us first analyze its ground- and excited-state geometric and electronic structures. The ground-state geometric parameters optimized at the different levels of theory are close to the experimental findings. The 30 electrons of the ground-state acrolein have a $(1a')^2\cdots(11a')^2(12a')^2(13a'')^2(14a')^2(15a'')^2$ electronic configuration. The two highest occupied π orbitals are located mainly at C3−O4 and C1−C2 σ bond regions, respectively. The latter is somewhat delocalized to the C3−O4 region. Such a feature of electronic structure was found in a previous study.[30] Because of the conjugation interaction between the C═C and C═O double bonds, the C2−C3 bond length is reduced by about 0.05 Å, compared with C−C bond length of CH_3CH_3.

The CAS(8,7)/cc-pVDZ-optimized geometries for the excited states are shown in Figure 1, where the atomic numbering is also given. From the geometric parameters in Figure 1a, it can be seen that the ^{3}nπ^* minimum is structurally similar to the ^{1}nπ^* minimum. The ^{1,3}nπ^* states possess C_s symmetry with all atoms in the molecular plane. These structures have been confirmed to be minima by the CAS(8,7)/cc-pVDZ-calculated frequencies, which are all real. The electronic rearrangements induced by excitation from the ground state to the ^{1,3}nπ^* states significantly influence the structures of acrolein. With respect to the ground state, the single/double character is almost interchanged in the ^{1,3}nπ^* states. The three-dimensional plots of some CAS(8,7)/cc-pVDZ-calculated active orbitals of ^{1}nπ^* state are depicted in Figure 1a, along with the CAS(8,7)/cc-pVDZ-calculated one-electron densities. The MO12 (the number represents the order of the molecular orbital) is a fully occupied C2−C3 σ orbital, and the corresponding antibonding orbital is the unoccupied MO17. The one-electron density in MO18 is nearly equal to zero. The other active orbitals shown in Figure 1a are the p_z (with the *xy* plane as a molecular plane) orbital of the O4 atom (MO13), the C2−C3 π orbital (MO14), the nonbonding orbital (MO15), and the antibonding π orbital (MO16). It should be noted that three active electrons are actually distributed in the O4 atom, namely, two in the p_z orbital and one in the n orbital. This distribution is different from that in the ground state, where two electrons are in the n orbital and one is in the C−O π orbital. Due to the inductive effect of the carbonyl group, it seems reasonable to expect that the initial excitation is a local transition from the n orbital to the C−O π^* orbital, which weakens to a large extent the C−O π bond. To stabilize system, the C2−C3 π bond is formed. Meanwhile, a conjugation interaction between the C2−C3 π electrons and the p_z electrons in C1 and O4 atoms results in a further stabilization of the system. It is the inductive and the conjugative effects that are responsible for the structural features of the ^{1,3}nπ^* states. Our CAS(8,7)/cc-pVDZ calculations predict that the ^{1,3}nπ^* states are planar, with an electron configuration of $\dot{C}H_2-CH{=}CH-\dot{O}$:. The excited-state molecular orbitals of *s-trans*-acrolein given by Arendt et al.[30] are similar to those reported here. It appears, however, that Arendt's group identified them as the orbitals of the $^1\pi\pi^*$ state.

The experimental values[47,48] of the 0−0 energies from the ground state to the ^{1}nπ^* and ^{3}nπ^* states were estimated to be 74 and 70 kcal/mol, respectively. The CAS(8,7)/cc-pVDZ calculations provide values of 71.3 and 68.7 kcal/mol, respectively. The deviation from the experimental results is not significantly improved by the CAS-PT2 calculations. As pointed out by Brand and Williamson,[15] the ^{1}nπ^* state is planar or nearly planar; an excitation from S_0 to ^{1}nπ^* increases the C−O distance by ca. 0.12 Å and effects a considerable redistribution of π electrons, so that a greater C−C bond order is associated with the central rather than the terminal C−C link. The CAS(8,7)/cc-pVDZ-calculated transition energies and optimized structures reproduce the above experimental findings quite well.

It seems clear that, while spectroscopic and theoretical investigations have provided an agreeable conclusion on the nπ^* states, there is still uncertainty regarding the $\pi\pi^*$ states. The structure of the $^3\pi\pi^*$ state is initially optimized with planar symmetry constraint. The resulting geometry is not a minimum point on the $^3\pi\pi^*$ surface. To relax to the minimum, an intramolecular rotation followed by a little distortion is required. In the optimized equilibrium structure, as shown in Figure 1b, all atoms are in the symmetry plane, except for H7 and H8, which lie symmetrically above and below the symmetry plane, respectively. The dihedral angles of H7−C1−C2−C3 and H8−C1−C2−C3 are 95.6° and −95.6°, respectively, at the CAS-(8,7)/cc-pVDZ level. Our optimized $^3\pi\pi^*$ structure is different from the early theoretical conclusion that the $^3\pi\pi^*$ state is planar[37,39] and also slightly different from the recently reported

(43) Dunning, T. H., Jr. *J. Chem. Phys.* **1989**, *90*, 1007.
(44) Frisch, M. J.; Trucks, G. W.; Schlegel, H. B.; Gill, P. M. W.; Johnson, B. G.; Robb, M. A.; Cheeseman, J. R.; Keith, T.; Petersson, G. A.; Montgomery, J. A.; Raghavachari, K.; Al-Laham, M. A.; Zakrzewski, V. G.; Ortiz, J. V.; Foresman, J. B.; Cioslowski, J.; Stefanov, B. B.; Nanayakkara, A.; Challacombe, M.; Peng, C. Y.; Ayala, P. Y.; Chen, W.; Wong, M. W.; Andres, J. L.; Replogle, E. S.; Gomperts, R.; Martin, R. L.; Fox, D. J.; Binkley, J. S.; Defrees, D. J.; Baker, J.; Stewart, J. P.; Head-Gordon, M.; Gonzalez, C.; Pople, J. A. *Gaussian 94*, Revision D.4; Gaussian, Inc., Pittsburgh, PA, 1995.
(45) Loncharich, R. J.; Schwartz, T. R.; Houk, K. N. *J. Am. Chem. Soc.* **1987**, *109*, 14.
(46) Wiberg, K. B.; Rosenberg, R. E.; Rablen, P. R. *J. Am. Chem. Soc.* **1991**, *113*, 2890.
(47) Alves, A. C. P.; Christoffersen, J.; Hollas, J. M. *Mol. Phys.* **1971**, *20*, 625.
(48) Inuzuka, K. *Bull. Chem. Soc. Jpn.* **1961**, *34*, 729.

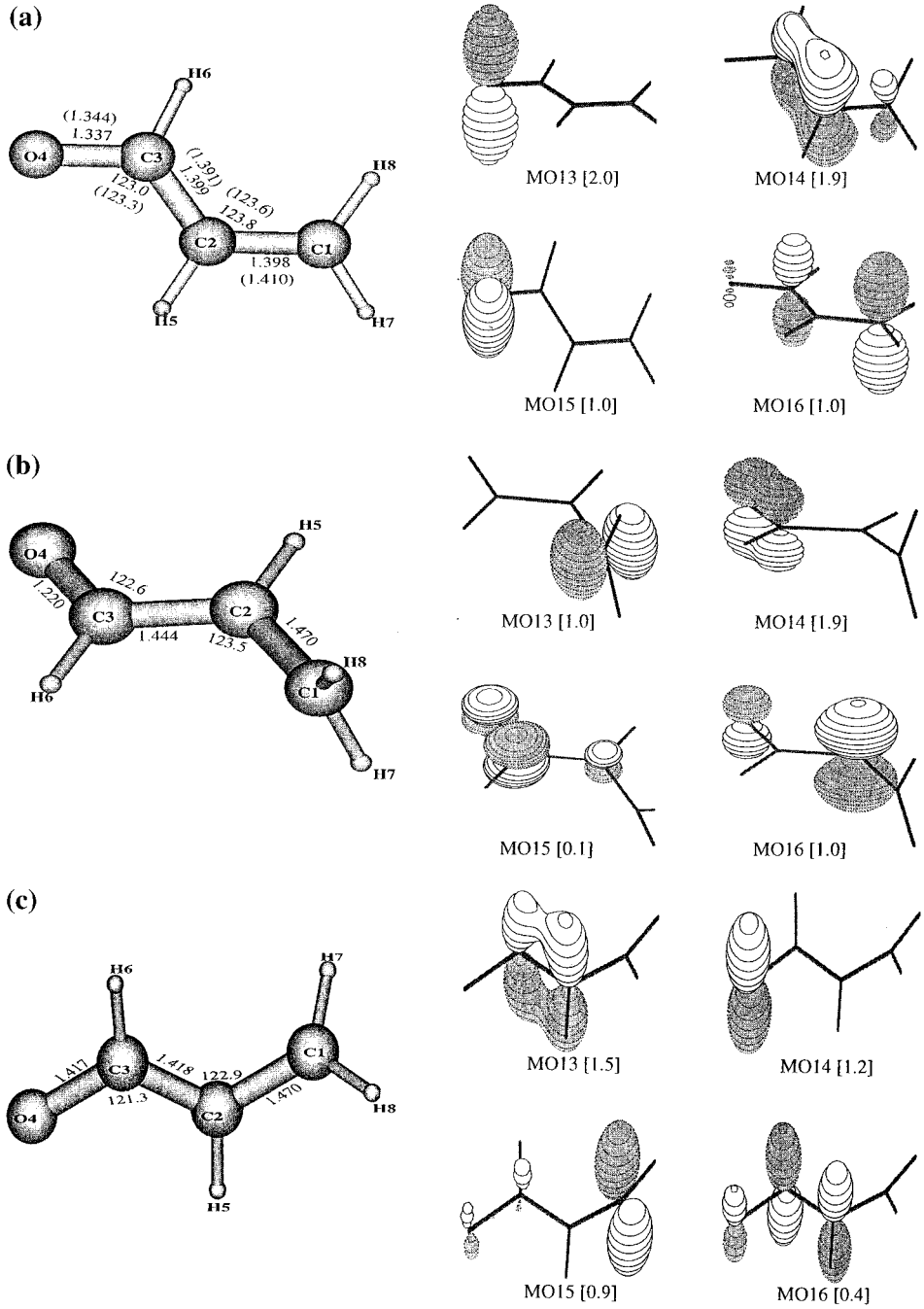

Figure 1. Schematic structures (bond lengths in angstroms and bond angles in degrees) and plots of some molecular orbitals (one-electron densities are given in square brackets): (a) the ^{1,3}nπ^* state (structural parameters of the ^{1}nπ^* state are given in parentheses), (b) the $^3\pi\pi^*$ state, and (c) the $^1\pi\pi^*$ state.

geometry,[42] in which the dihedral angle H7−C1−C2−C3 was restricted to be 90° (perpendicular structure).

The CAS(8,7)/cc-pVDZ-calculated molecular orbitals can provide a better picture for the electronic structure of the $^3\pi\pi^*$ state. The three-dimensional plots of the four active molecular orbitals, MO13, MO14, MO15, and MO16, are presented in Figure 1b, along with the CAS(8,7)/cc-pVDZ-calculated one-electron densities. From Figure 1b it is reasonable to expect that the $^3\pi\pi^*$ state has the form of $\dot{C}H_2-\dot{C}H-CH=O$ that has been somewhat modified by a charge-transfer configuration. One electron is initially excited from the π to π^* orbital, which makes the C1−C2 π bond nearly broken. In this case, the bond between C1 and C2 atoms is mainly of single bond character, and the terminal CH_2 group can more easily rotate around the C1−C2 bond, leading to the perpendicular structure. A little distortion from the perpendicular structure takes place due to an unsymmetric distribution of the atoms with respect to the terminal CH_2 group. The conjugation interaction between the p_z electron of C2 atom and the C3−O4 π electrons results in a further stabilization of the system.

The $^1\pi\pi^*$ minimum is usually difficult to optimize, since it is not the lowest state of its symmetry. The $^1\pi\pi^*$ surface has been calculated on a regular grid over rotations of the terminal CH_2 and CHO groups from 180° to 90° with a step size of 5°. Meanwhile, the relaxations of the C−C and C−O distances as well as the C1−C2−C3 and C2−C3−O4 angles are considered. Finally, an energy minimum is found with the CH_2 and CHO groups twisted about 125° and 5°, respectively, as shown in Figure 1c. The four important active orbitals, MO13, MO14, MO15, and MO16, are also depicted in Figure 1c, along with

their one-electron densities from the CAS(8,7)/cc-pVDZ calculations. It is evident that the doubly excited configurations from the C=C and C=O π orbitals to their antibonding orbitals make a main contribution to the $^1\pi\pi^*$ state. Because of the inductive effect, an electron migrates partially toward the O4 atom. The CAS(8,7)/cc-pVDZ-calculated atomic charge is about -0.2 on the O4 atom, i.e., the following backbone structure dominates in the $^1\pi\pi^*$ state:

$$\overset{\delta+}{C}-C\cdots C-\overset{\delta-}{O}$$

The charge-transfer configurations were found to make an important contribution to the $^1\pi\pi^*$ state by a semiempirical molecular orbital calculation.[49] Some previous calculations[30,35−40] were carried out with most bond parameters fixed at the ground-state values, thus predicting the planar or perpendicular structure to be a minimum point on the $^1\pi\pi^*$ surface. The CAS(8,7)/cc-pVDZ calculations here show that the equilibrium geometry of the $^1\pi\pi^*$ state has no symmetry. The vertical excitation energy to this state, obtained at the CAS(8,7)/cc-pVDZ level, is about 191 kcal/mol, which is 41 kcal/mol higher than the observed value of 150 kcal/mol. The deviation from the experimental finding is reduced to 19.2 kcal/mol with the effect of dynamic electron correlation considered at the CAS-PT2[50] level. This result is better than that from configuration interaction calculations,[40] which gave a vertical excitation energy of 7.5 eV (173 kcal/mol) to the $^1\pi\pi^*$ state.

An analysis of the low-lying electronic states of the intermediates and some products can give us some help in understanding the mechanism of the photodissociation. The CAS(4,5)/cc-pVDZ calculations predict the ground-state methylcarbene to be of C_1 symmetry, which is well consistent with a recent calculation by Ma and Schaefer.[51] In addition, the ground state of methylcarbene is actually of closed-shell character. This can be clearly seen from the CAS(4,5)/cc-pVDZ-calculated one-electron densities. The lowest triplet of methylcarbene (^{3}A″) is of C_s symmetry. This state lies 1.6 kcal/mol in energy above the ground state, predicted by the CAS(4,5)/cc-pVDZ calculations with zero-point energy correction. The singlet−triplet energy separation was predicted to be in the range of 4−35 kcal/mol by the previous calculations.[52] These calculations have been carried out under the condition that the triplet state is the ground state, thus predicting different singlet−triplet energy separation from the value reported here. The first excited singlet state of methylcarbene is of ^{1}A″ symmetry. However, the energy minimum for CH_3CH was not found on the ^{1}A″ surface.

The optimized structures of the lowest three states of methylketene are depicted in Figure 2. Similar to the ground-state geometry of ketene, a linear configuration, C2−C3−O4, is found for the ground-state methylketene. One-electron excitation from the C2−C3 π bonding orbital to its antibonding orbital results in a breaking of the C2−C3 π bond. Meanwhile, a rehybridization of the C3 atom from sp to sp^2 takes place. As a consequence of this, the C2−C3 bond is mainly of single bond character in the triplet (^{3}A″) and excited singlet (^{1}A″) states of methylketene with a bent C2−C3−O4 configuration. The ground state of CH_2CHCO is a planar structure of ^{2}A′ symmetry. The highest singly occupied orbital is the p_y atomic orbital of the C3 atom, and the C1=C2 and C3=O4 double bonds are similar to those in ground-state acrolein. The first excited state of CH_2CHCO is also a planar structure, but with ^{2}A″ symmetry. One-electron excitation from the C1−C2 π bond to its antibonding orbital leads to a redistribution of π electrons. An allene-like structure ($CH_2CH=C=O$) is produced with one electron in the p_z atomic orbital of the C1 atom. All of these can be clearly seen from the CAS(7,6)/cc-pVDZ-optimized ^{2}A′ and ^{2}A″ structures in Figure 2 and calculated molecular orbitals.

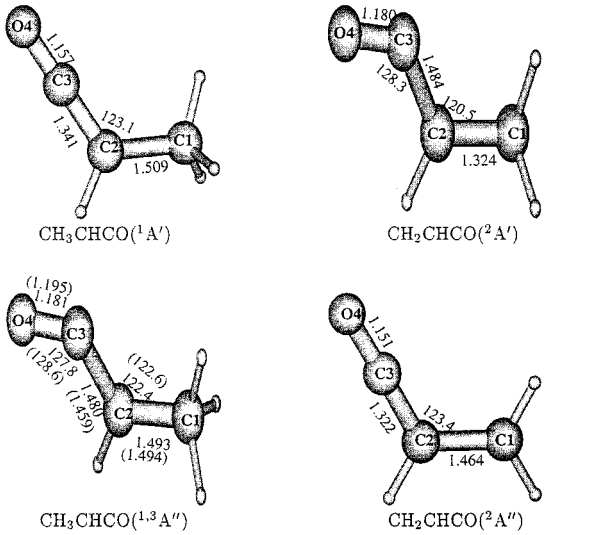

Figure 2. Schematic structures (bond lengths in angstroms and bond angles in degrees) of the low-lying electronic states of CH_2CHCO and CH_3CHCO (structural parameters of $CH_3CHCO(^1A'')$ are given in parentheses).

B. Decarbonylation Reaction: $CH_2CHCHO \rightarrow CH_2CH_2 + CO$. The photodissociation of acrolein is probably nonadiabatic. The reaction starts on an excited-state surface and may proceed ultimately on the ground-state surface. An accurate knowledge of the ground-state potential energy profile is required in describing mechanistic photochemistry. The ground-state decarbonylation of acrolein is an elemental reaction. Geometries of the reactant, transition state, and products on the decarbonylation pathway are optimized using the MP2, CAS-(8,7), and QCISD methods. The CAS(8,7)/cc-pVDZ-optimized structure of the transition state (TS_G) is shown in Figure 3, where the bond parameters are also given. On the basis of the calculated energies given in the Supporting Information, the potential energy profile of the ground-state decarbonylation is depicted in Figure 4. The decarbonylation reaction is exothermic by 0.6 kcal/mol at the CAS(8,7)/cc-pVDZ and QCISD/cc-pVDZ levels with the zero-point vibrational energy correction, while at the MP2/cc-pVDZ level the reaction is exothermic by 3.1 kcal/mol. As pointed out by Huber and co-workers,[29] the almost thermoneutral molecular reaction of acrolein gives rise to $CH_2=CH_2$ and CO. The energy difference calculated at three different levels is close to the experimental data. This provides a good indication of the overall accuracy of our calculations. The barrier height on the ground-state decarbonylation pathway is calculated to be 93.3, 93.9 and 90.8 kcal/mol at the CAS(8,7)/cc-pVDZ, QCISD/cc-pVDZ, and MP2/cc-pVDZ levels, respectively. With the zero-point vibrational energy correction, they become 88.7, 89.3, and 86.2 kcal/mol, respectively. A final estimate of 85.0 kcal/mol for the barrier height is obtained with the CAS-PT2 calculations based on the CAS(8,7)/cc-pVDZ-optimized structures. Due to a high barrier on the ground-state pathway, there is little possibility that the thermodecarbonylation of acrolein

(49) Nagakura, S. *Mol. Phys.* **1960**, *3*, 105.
(50) McDouall, J. J.; Peasley, K.; Robb, M. A. *Chem. Phys. Lett*. **1988**, *148*, 183.
(51) Ma, B.; Schaefer, H. F. *J. Am. Chem. Soc.* **1994**, *116*, 3539.
(52) Gallo, M. M.; Schaefer, H. F. *J. Phys. Chem.* **1992**, *96*, 1515 and references therein.

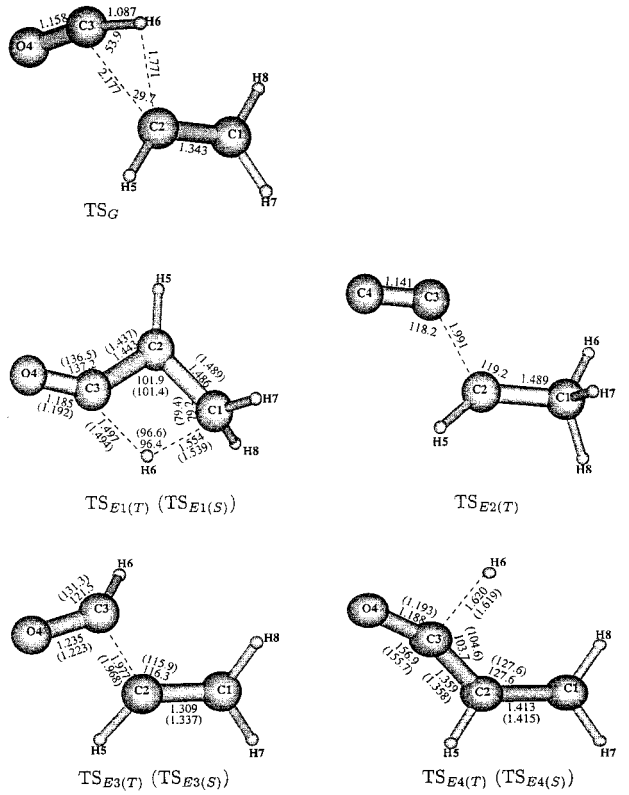

Figure 3. Schematic structures (bond lengths in angstroms and bond angles in degrees) of the transition states (structural parameters of the singlet transition states are given in parentheses).

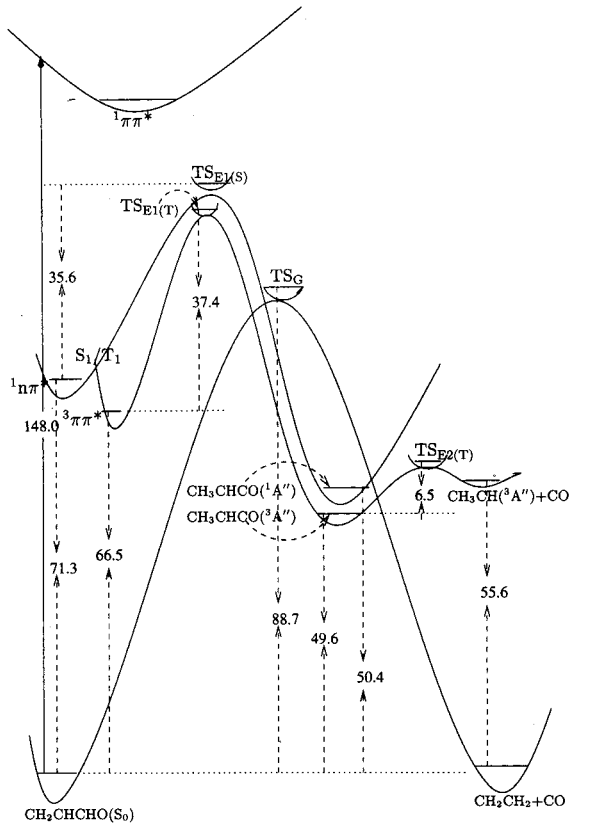

Figure 4. Schematic potential energy profiles of the decarbonylation reaction; relative energies are given in kcal/mol. The ground- and excited-state potential energy profiles do not intersect in both sides of the ground-state barrier, since they correspond to different nuclear geometries.

occurs under normal conditions. To our knowledge, the thermodecarbonylation was not experimentally documented in the literature.

In comparison with the CAS-PT2 approach, the QCISD calculations overestimate slightly the barrier height, whereas the MP2 barrier height is very close to that calculated at the CAS-PT2 level. This shows that dynamic electron correlation is mainly included in the single-reference MP2 calculations. Although the CAS-PT2 is a very efficient algorithm for treating dynamic electron correlation, since the position of the barrier is more sensitive to the electron correlation method used than the equilibrium geometry, the single-point CAS-PT2 calculations (without optimization) cause some errors which decrease the overall accuracy of the calculated barrier height. This is also one reason the 0−0 energies reported above were changed only a little on going from CASSCF to CAS-PT2. Geometry is not changed in a vertical excitation process; thus, the CAS-PT2 vertical excitation energy to the $^1\pi\pi$ state is very close to the experimental value, as given before.

The ^{3}nπ^* state is planar, so there is little possibility that a migration of the H6 atom to the C1 atom occurs within the plane, due to steric effects. Unlike the ^{3}nπ^* state, the twisted equilibrium geometry of the $^3\pi\pi^*$ state provides a good opportunity for the H6 migration to the C1 atom, which gives us a hint that the photodecarbonylation reaction of acrolein probably starts from the $^3\pi\pi^*$ state. The reaction involves a two-step mechanism, namely, isomerization to methylketene (CH_3CHCO) through a transition state ($TS_{E1(T)}$), followed by dissociation into the products CH_3CH + CO via the second transition state ($TS_{E2(T)}$). The CAS(8,7)/cc-pVDZ-optimized structures of $TS_{E1(T)}$ and $TS_{E2(T)}$ are shown in Figure 3, along with their structural parameters. In the triplet transition state $TS_{E1(T)}$, the bond between H6 and C1 is partially formed, and the H6−C3 bond is partially broken. The analysis of the eigenvector corresponding to the negative eigenvalue of the force constant matrix indicates that the internal coordinate reaction vector is mainly composed of the H6−C3 bond cleavage and a change in the H6−C3−C2 and C1−C2−C3 angles. The reaction vector corresponding to the imaginary frequency (2470i cm^{-1}) has been identified as $0.4R_{H6-C3} - 0.5A_{H6-C3-C2} - 0.4A_{C1-C2-C3}$. It is obvious that $TS_{E1(T)}$ is the transition state governing a migration of the H6 atom from the C3 to the C1 atom. There is a barrier of 37.4 kcal/mol on the first step of the triplet decarbonylation pathway, as shown in Figure 4. This process is reinvestigated at the MP2/cc-pVDZ level. The resulting barrier is 33.4 kcal/mol, 4.0 kcal/mol lower than that of the CAS(8,7)/cc-pVDZ calculations. This gives a hint how dynamic electron correlation affects the calculated barrier height. The second step of the triplet pathway involves a breaking of the C2−C3 bond, forming $CH_3CH(^3A'')$ and CO-($^1\Sigma^+$). A transition state is optimized and confirmed to be the first saddle point ($TS_{E2(T)}$) by the CAS(8,7)/cc-pVDZ calculations. With respect to $CH_3CHCO(^3A'')$, the barrier height is 6.5 kcal/mol, which is much lower than that on the first step of the isomerization.

A transition state of $^1A''$ symmetry, referred to as $TS_{E1(S)}$, which is structurally similar to $TS_{E1(T)}$, is found on the first excited singlet isomerization pathway to $CH_3CHCO(^1A'')$. From the imaginary vibrational modes, it can be deduced that, on the reactant side, $TS_{E1(S)}$ should connect a structure which is similar to $CH_2CHCHO(^3\pi\pi^*)$. A rotation of the terminal CH_2 group around the C1−C2 bond is required before the isomerization from $CH_2CHCHO(^1n\pi^*)$ to $CH_3CHCO(^1A'')$. Since the C1−C2 bond in $CH_2CHCHO(^1n\pi^*)$ is mainly of single bond character, the terminal CH_2 group twists easily. The barrier

height is 35.6 kcal/mol with respect to the $CH_2CHCHO(^1n\pi^*)$ zero-point level. From the viewpoint of symmetry, $CH_3CHCO(^1A'')$ can correlate adiabatically with $CH_3CH(^1A'') + CO(^1\Sigma^+)$. Since the stable $CH_3CH(^1A'')$ structure was not found, there is no transition state on this pathway.

As a general rule, regardless of which of the excited states are initially populated by photoexcitation, reactions normally proceed on the ground or lowest excited singlet and triplet surfaces, especially for polyatomic molecules.[53] The $^1\pi\pi^*$ state correlates adiabatically with highly excited states of the products, $CH_3CH + CO$, $CH_2CH + CHO$, or $CH_2CHCO + H$, which are not energetically accessible even with photoexcitation at 193 nm (148 kcal/mol). Therefore, one can eliminate the possibility of adiabatic dissociation from the $^1\pi\pi^*$ state. In their study of the laser photofragmentation dynamics of acrolein at 193 nm, Shinohara and Nishi[26] pointed out that the $\pi-\pi^*$ excitation does not open the channel for the observed dissociation. With respect to the $CH_2CHCHO(S_0)$ zero-point level, the barrier of isomerization to methylketene is 106.9 kcal/mol on the first excited singlet pathway, which is 3 kcal/mol higher than the corresponding barrier on the lowest triplet pathway, while the barrier is 88.7 kcal/mol on the ground-state decarbonylation pathway. It is favorable in energy that the photodecarbonylation of acrolein ultimately takes place on the ground-state surface.

The $S_0/S_1(^1n\pi^*)$ conical intersection point occurs at a perpendicular structure with the terminal CH_2 group twisted 90° and lies about 15 kcal/mol in energy above the $^1n\pi^*$ minimum.[42] This conical intersection point is about 20 kcal/mol in energy below the barrier of the isomerization on the S_1 pathway. If the terminal CH_2 group twists 90°, the resulting perpendicular structure will not isomerize to $CH_3CHCO(^1A'')$ along S_1 pathway and instead decays to the ground state of acrolein via the S_0/S_1 intersection point. However, the $^1n\pi^*/^3\pi\pi^*$ crossing point occurs at a planar geometry which is structurally close to the $^1n\pi^*$ minimum. This crossing point is just 4 kcal/mol above the energy of the $^1n\pi^*$ minimum.[42] An intersystem crossing from the $^1n\pi^*$ to the $^3\pi\pi^*$ state is usually assumed to occur with high efficiency.[54,55] It can be expected that the intersystem crossing to the $^3\pi\pi^*$ state takes place much more easily than does decay to the ground state via the S_0/S_1 point. After photoexcitation at 193 nm, *s-trans*-acrolein relaxes to the $^1n\pi^*$ state. From this state, the system decays to the $^3\pi\pi^*$ state through the $^1n\pi^*/^3\pi\pi^*$ crossing point, followed by isomerization to $CH_3CHCO(^3A'')$. The dissociation of the formed $CH_3CHCO(^3A'')$ takes place very easily, due to a small barrier on the way to the products $CH_3CH(^3A'') + CO(^1\Sigma^+)$. Ha et al.[56] had proposed that triplet methylcarbene, although a local minimum on the surface, does not exist as a stable species. It will undergo intersystem crossing to the singlet surface and immediately transform to the ground-state ethylene. The most probable mechanism of the CH_2CHCHO photodecarbonylation is that the excited CH_2CHCHO molecules first relax to the $^3\pi\pi^*$ state and then isomerize to $CH_3CHCO(^3A'')$, followed by its dissociation into $CH_3CH(^3A'') + CO(^1\Sigma^+)$ along the lowest triplet pathway, and $CH_2CH_2 + CO(^1\Sigma^+)$ are finally formed.

C. Norrish Type I Reaction: $CH_2CHCHO \rightarrow CH_2CH + CHO$. The ground-state CH_2CH and CHO are both planar radicals with $^2A'$ symmetry. When the two radicals approach each other in-plane, they can correlate adiabatically with the ground-state acrolein. We attempt to optimize a transition state on the ground-state pathway with the CAS(8,7)/cc-pVDZ approach. The energy gradient ($\partial E/\partial R_{C-C}$) increases gradually to -0.0004 E_h/å with the growth of the C2−C3 distance to the dissociation limit. The saddle point search does not converge but instead leads to the dissociation products $CH_2CH(^2A')$ and $CHO(^2A')$. This shows that no transition state exists on the dissociation pathway of $CH_2CHCHO(S_0)$ into $CH_2CH(^2A')$ and $CHO(^2A')$. The reaction is endothermic by 90.7 kcal/mol at the CAS(8,7)/cc-pVDZ level. With vibrational zero-point energy correction, it becomes 84.4 kcal/mol, which is lower than the experimental estimate of 96.4 kcal/mol.[29]

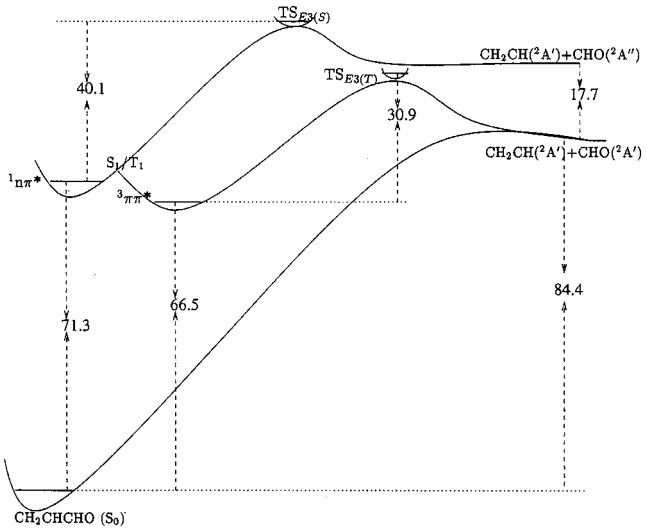

Figure 5. Schematic potential energy profiles of the CH_2CHCHO dissociation into $CH_2CH + CHO$; relative energies are given in kcal/mol.

The lowest triplet surface of acrolein along the pathway of nuclear geometries that leads to dissociation to $CH_2CH + CHO$ can be viewed as originating from the interaction of an excited $^3\pi\pi^*$ configuration and a locally excited $^3\sigma\sigma^*$ configuration of the C2−C3 bond. The former is lower in energy at the initial geometry, as is the latter at the final geometries. Somewhere along the way they intend to cross, but the crossing is avoided and results in a barrier separating the two minima on the lowest triplet surface, as depicted in Figure 5. The barrier existence is confirmed by the CAS(8,7)/cc-pVDZ calculations. The CAS(8,7)/cc-pVDZ-optimized transition state ($TS_{E3(T)}$) of the lowest triplet dissociation to $CH_2CH + CHO$ does not possess any symmetry, as schematically shown in Figure 3. At the CAS(8,7)/cc-pVDZ level, the barrier height is calculated to be 30.9 kcal/mol with respect to the $CH_2CHCHO(^3\pi\pi^*)$ zero-point level. In $TS_{E3(T)}$ the C2−C3 bond is nearly broken, and the structures of the CHO and CH_2CH moieties are similar to the corresponding ground-state products. It can be seen from $TS_{E3(T)}$ that, in the case of the reverse process of the dissociation, the radicals CHO and CH_2CH do not approach in-plane but are nearly perpendicular to each other. The barrier of the reverse reaction is about 13 kcal/mol.

Using the CAS(8,7)/cc-pVDZ-optimized nonplanar structure and calculated molecular orbitals of the transition state ($TS_{E3(T)}$) as an initial guess, the structure of $TS_{E3(S)}$ on the first excited singlet pathway is optimized at the same level. From the displace vectors associated with the imaginary vibrational modes of $TS_{E3(S)}$, it can be deduced that $TS_{E3(S)}$ is the transition state connecting the $CH_2CHCHO(^1n\pi^*)$ reactant and the excited-state products $CH_2CH(^2A')$ and $CHO(^2A'')$. The adiabatic excitation energy from $HCO(^2A')$ to $HCO(^2A'')$ is 17.7 kcal[29] (0.8 eV),

(53) Portner, J.; Rice, S. A. *Adv. Photochem.* **1969**, *7*, 149.
(54) Zimmerman, H. E. *Tetrahedron* **1974**, *30*, 1617.
(55) Turro, N. J. *Modern Molecular Photochemistry*; Benjamin/Cummings: Menlo Park, CA, 1978.
(56) Ha, T. K.; Nguyen, M. T.; Vanquickenborne, L. G. *Chem. Phys. Lett.* **1982**, *92*, 459.

which is much lower than that from $CH_2CH(^2A')$ to $CH_2CH(^2A'')$, 2.4 eV[57] (55.3 kcal/mol). These show that acrolein in the $^1n\pi^*$ state dissociates adiabatically into the first excited singlet state of the products, which is consistent with a prediction by state correlation. The barrier height, calculated at the CAS(8,7)/cc-pVDZ level, is 40.1 kcal/mol with respect to the $CH_2CHCHO(^1n\pi^*)$ zero-point level. The dissociation of CH_2CHCHO into $CH_2CH + CHO$ is endothermic, and the transition states are structurally closer to their corresponding products, which is well consistent with Hammond's postulate:[58] the endothermic reaction has a transition-state geometry close to that of the product.

The products CH_2CH and CHO have been found by Coomber and Pitts[25] upon 313-nm photodissociation of acrolein. The corresponding vertical excitation energy to the $^1n\pi$ state is about 92 kcal/mol. With respect to the zero-point level of the ground-state acrolein, the barrier height on the first excited singlet pathway is 111.4 kcal/mol, which is 19.4 kcal/mol above the vertical excitation energy. This shows that the dissociation of $CH_2CHCHO(^1n\pi^*)$ into $CH_2CH(^2A') + CHO(^2A'')$ is impossible, since it is not energetically accessible at 313-nm photoexcitation. The barrier on the lowest triplet pathway to the products $CH_2CH(^2A') + CHO(^2A')$ is only about 2 kcal/mol higher than the dissociation limit, and the $^1n\pi^*/^3\pi\pi^*$ intersystem crossing takes place much more easily than the internal conversion to the ground state. Therefore, the dissociation to the ground-state products $CH_2CH(^2A') + CHO(^2A')$ mainly proceeds along the lowest triplet pathway, although no energy barrier above endothermicity is found for the ground-state dissociation.

D. The C−H α-Cleavage Reaction: $CH_2CHCHO \rightarrow CH_2CHCO + H$. Similar to the ground-state process, $CH_2CHCHO \rightarrow CH_2CH + CHO$, no energy barrier above endothermicity is found on the ground-state dissociation pathway of CH_2CHCHO into $CH_2CHCO + H$. The reaction is endothermic by 90.5 kcal/mol at the CAS(8,7)/cc-pVDZ level; with vibrational zero-point energy correction, it becomes 83.2 kcal/mol, a value close to the experimental estimate of 87.1 kcal/mol.[59] The ground state of CH_2CHCO is a planar radical with $^2A'$ symmetry. This state, together with the ground-state H atom (^2S), can correlate with the ground and $^3\pi\pi^*$ states of acrolein. A planar transition state ($TS_{E4(T)}$) on the triplet pathway is found, as shown in Figure 3. Based on the calculated molecular orbitals, structural parameters, and the displace vectors associated with the imaginary vibrational modes, it can be seen that $TS_{E4(T)}$ is the transition state connecting the $CH_2CHCHO(^3n\pi^*)$ reactant and the first excited triplet products $CH_2CHCO(^2A'') + H(^2S)$. With respect to the $CH_2CHCHO(^3n\pi^*)$ zero-point level, the barrier height is calculated to be 30.1 kcal/mol at the CAS(8,7)/cc-pVDZ level and 26.3 kcal/mol at the MP2/cc-pVDZ level. As in the isomerization to $CH_3CHCO(^3A'')$ from $CH_2CHCHO(^3\pi\pi^*)$, the barrier height is reduced by about 4 kcal/mol with dynamic electron correlation correction. The products $CH_2CHCO(^2A'') + H(^2S)$ can also correlate adiabatically with the $^1n\pi^*$ state. A planar transition state ($TS_{E4(S)}$), very similar to $TS_{E4(T)}$, is found on the $^1A''$ pathway. With respect to the $^1n\pi^*$ minimum, the barrier height is 28.9 kcal/mol. The potential energy profiles of the dissociation to $CH_2CHCO + H$ are shown in Figure 6. The C−H α-cleavage reaction of acrolein has been studied by Reinsch and co-workers[60] with the semiempirical MNDOC-CI method. A barrier of about 43 kcal/mol was found in their study. Since the $^3\pi\pi^*$ structure was constrained to be planar and the O−C−C angle fixed at 130°, the obtained barrier is only qualitatively reliable. All attempts to search a nonplanar transition state on the lowest triplet surface led to the planar $TS_{E4(T)}$, which is confirmed to connect the $CH_2CHCHO(^3n\pi^*)$ reactant and the excited-state products. The electronic and geometric structures of $CH_2CHCO(^2A')$ are quite different from those of the CH_2CHCO moiety in $CH_2CHCHO(^3\pi\pi^*)$, while the H atom departure does not have a large influence on the structure of the CH_2CHCO moiety. It can be expected that a large barrier exists on the dissociation pathway from $CH_2CHCHO(^3\pi\pi^*)$ to $CH_2CHCO(^2A') + H(^2S)$. To the contrary, the dissociation from $CH_2CHCHO(^3n\pi^*)$ to $CH_2CHCO(^2A'') + H(^2S)$ involves only the H atom departure in-plane, and hence, a small change in the structure is required in this process. The reaction from $CH_2CHCHO(^3n\pi^*)$, therefore, proceeds more easily, compared with the dissociation from $CH_2CHCHO(^3\pi\pi^*)$.

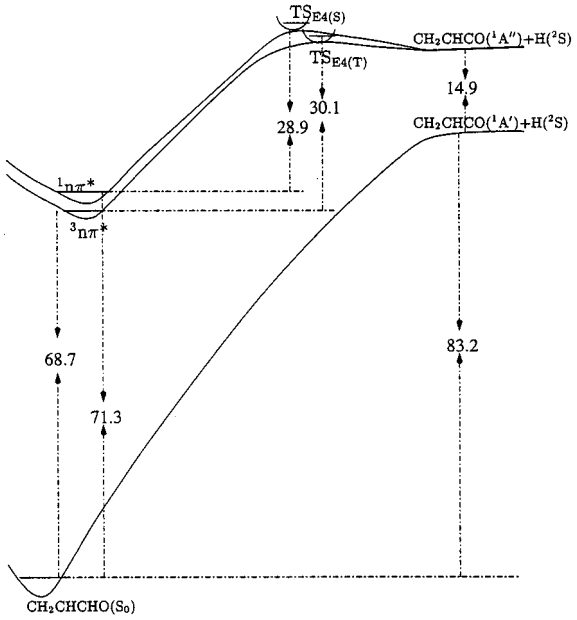

Figure 6. Schematic potential energy profiles of the CH_2CHCHO dissociation into $CH_2CHCO + H$; relative energies are given in kcal/mol.

In addition to correlating with the excited-state products, larger barriers exist on the $^{1,3}A''$ dissociation pathways starting from $CH_2CHCHO(^{1,3}n\pi^*)$. Generally speaking, an intersystem crossing from $^1n\pi^*$ to $^3n\pi^*$ occurs with very low efficiency in the carbonyl compounds.[55] Although the intersystem crossing from $^1n\pi^*$ to $^3\pi\pi^*$ state takes place more easily than internal conversion to the ground state, the dissociation of $CH_2CHCHO(^3\pi\pi^*)$ into $CH_2CHCO(^2A') + H(^2S)$ is difficult to induce. After photoexcitation at 193 nm, the CH_2CHCHO molecules that relaxed to the $^1n\pi^*$ state will return to the ground state via the S_0/S_1 intersection point. The dissociation ultimately proceeds on the ground-state surface. This is the most probable mechanism of the CH_2CHCHO photodissociation to the ground-state products $CH_2CHCO(^2A') + H(^2S)$.

4. Summary

The geometric and electronic structures of the low-lying electronic states of acrolein, methylketene, methylcarbene, and

(57) Hunziker, H. E.; Kneppe, H.; McLean, A. D.; Siegbahn, P.; Wendt, H. R. *Can. J. Chem.* **1983**, *61*, 993.

(58) Hammond, G. S. *J. Am. Chem. Soc.* **1955**, *77*, 334−338.

(59) Alfassi, Z. B.; Golden, D. M. *J. Am. Chem. Soc.* **1973**, *95*, 319.

(60) Reinsch, M.; Howeler, U.; Klessinger, M. *J. Mol. Struct. (THEOCHEM)* **1988**, *167*, 307.

the CH_2CHCO radical are determined by the CASSCF computations. The potential energy profiles, governing the dissociation of CH_2CHCHO to $CH_3CH + CO$, $CH_2CH + CHO$, and $CH_2CHCO + H$ in the ground state as well as in the excited singlet and triplet states, are traced at different levels with the cc-pVDZ basis set, as summarized in Figures 4−6. The most probable mechanism leading to different products is characterized on the basis of the obtained potential energy profiles and their crossing points. Acrolein excited to the $^1\pi\pi^*$ state first relaxes to the $^1n\pi^*$ state. From this state, acrolein can decompose into the products via three different routes. The first route involves radiationless decay to the ground state, leading to the production of $CH_2CHCO(^2A')$ and $H(^2S)$. The second route involves intersystem crossing to the $^3\pi\pi^*$ state, followed by dissociation to the ground-state products $CH_2CH(^2A') + CHO(^2A')$. Also, the acrolein molecules populated in the $^3\pi\pi^*$ state can isomerize to $CH_3CHCO(^3A'')$, which dissociates easily into $CH_3CH(^3A'') + CO(^1\Sigma^+)$. The formed $CH_3CH(^3A'')$ immediately transforms to the ground-state ethylene. This is the third route of the CH_2CHCHO decarbonylation. Since $^1n\pi^*/^3\pi\pi^*$ intersystem crossing occurs more easily than internal conversion to the ground state, the latter two routes take place with higher efficiency than the first route. The decarbonylation from the $^3\pi\pi^*$ state is a multistep process. To overcome the barrier on the first step, more energy is required, compared with the dissociation to $CH_2CH(^2A') + CHO(^2A')$. Of the three routes, the dissociation of CH_2CHCHO into $CH_2CH(^2A') + CHO(^2A')$ proceeds most easily. Finally, it should be pointed out that rate of the CH_2CHCHO photodissociation is not calculated here, since it requires a rather complex dynamics treatment and such a determination is not a purpose of the present paper.

Acknowledgment. This work has been supported by the Alexander von Humboldt Foundation of Germany and the National Natural Science Foundation of China (Grant No. 29673007).

Supporting Information Available: Geometric parameters, energies, and vibrational frequencies of the reactant, intermediates, transition states, and some products (PDF). This material is available free of charge via the Internet at http://pubs.acs.org.

JA982334I